ONLINE ISSN 2069-7430
ISSN-L 1841-4737

PRO LIGNO
www.proligno.ro

Vol. 9 N° 4 2013
pp. 50-59

DESIGN OF LARGE RECTANGULAR HOLES IN COMPRESSION AND MOMENT LOADED GLULAM MEMBERS

Simon AICHER
Dr. – Material Testing Institute University of Stuttgart – Department Timber Constructions
Address: Pfaffenwaldring 4 b, 70569 Stuttgart, Germany
E-mail: simon.aicher@mpa.uni-stuttgart.de

Nikola ZISI
Ph.D. – Material Testing Institute University of Stuttgart – Department Timber Constructions
Address: Pfaffenwaldring 4 b, 70569 Stuttgart, Germany
E-mail: zisi.nikola@mpa.uni-stuttgart.de

Abstract:

Holes represent a frequent construction necessity in load bearing members irrespective of the employed building material. Contrary to steel and reinforced concrete, holes in glued laminated timber beams, termed glulam, pose a delicate detailing and design task. The problems emanate from the expressed orthotropicity of the wooden material characterized by very low stiffness and tensile strength values perpendicular to the fiber direction. The complexity of the mechanical problem is the reason why the European code for design of timber structures, Eurocode 5 (EC5), so far does not contain any detailing and design provisions for holes in glulam beams. Contrarily, however, some national codes do give such design equations.

The paper deals with design relevant stress distributions in the periphery of rectangular holes in glulam members. Hereby, actions of bending moment M and shear force V as well as an axial compression force N are considered. Firstly, the stress distributions bound to M and V loading are considered whereby the basics of the present design approach given in the German national application document to EC5 are discussed. Secondly, and not treated previously in any known design provisions, the stress fields resulting from axial compression loading are considered. Hereby, i.a. the effects of the hole size relative to the beam depth and of the constitutive law are quantified. It is shown that axial compression loading of a rectangular hole in glulam leads to very high tensile stresses perpendicular to the fiber direction along the vertical hole edges which may in turn lead to cracking parallel to the fiber direction. Furthermore, the concentration of compression stresses parallel to the fiber direction along the horizontal hole edges is far more pronounced as in the case of an isotropic material, possibly motivating the necessity to consider the yielding potential of timber in compression parallel to the fiber direction. The interaction of moment, shear and compression loading of square holes can be handled in a first approach by the equations derived in the paper.

Key words: *glulam; rectangular holes; axial compression; moment and shear force action; stress distributions; design equations.*

ONLINE ISSN 2069-7430
ISSN-L 1841-4737
PRO LIGNO
www.proligno.ro
Vol. 9 N° 4 2013
pp. 50-59

INTRODUCTION

Holes represent a frequent construction necessity in beams to enable the passing of cables or tubes for electricity, ventilation or sewage water. This demand is irrespective of the construction material, which may be wood, reinforced concrete or steel. For both of the latter mentioned materials, the placement of holes poses rather few problems with regard to the load capacity of the beams. In case of reinforced concrete, additional reinforcement bars can be easily integrated to transfer the stress flow around the hole. In case of steel beams, the advantages of material isotropy and elastic plastic behavior enable fairly large web holes without reinforcement which can be easily applied through welding when necessary. With respect to wood however, the highly anisotropic material behavior and most notably the very low tensile strength perpendicular to the fiber direction poses considerably more problems. As large timber constructions with necessities for holes are predominantly executed with glulam beams, this glued solid wood product is considered here.

Currently, Eurocode 5 (EN 1995-1-1:2010), henceforth termed EC5, does not contain any design or reinforcement provisions for glulam beams with holes. In contrast, the German national application document to EC5 (DIN EN 1995-1-1/NA:2010), henceforth termed EC5/NA, gives constructive rules for sizes, edge and support distances of round and rectangular holes in unreinforced and reinforced states and the respective design equations. However, the design is exclusively related to holes in beams subjected to the actions of bending moment and shear force. Although this covers the predominant construction needs, as holes occur most often in members for roofs or ceilings subjected to bending, there are design situations where superimposed normal stresses parallel to the beam or column axis have to be considered. These situations occur i.a. in column and beam parts of portal frames and in 2- or 3- hinged frames where the support reactions are carried by steel tensile chords inducing compression forces in the members.

This paper addresses square holes in straight glulam beams subjected to axial compression forces acting in addition to bending moment and shear force actions. Basic stress distributions are depicted and first design proposals are presented in the following.

GEOMETRY NOTATIONS AND SECTION FORCES

Fig. 1 shows a beam or column with a rectangular hole and the respective dimensional notations as well as the sections relevant for design verification. Further, the section forces - bending moment M, shear force V and compression force N acting on the beam in the vicinity of the hole are given. While the bending moment and shear force may have opposite orientations than the ones shown in the figure, the action of the axial force is always assumed to be in compression.

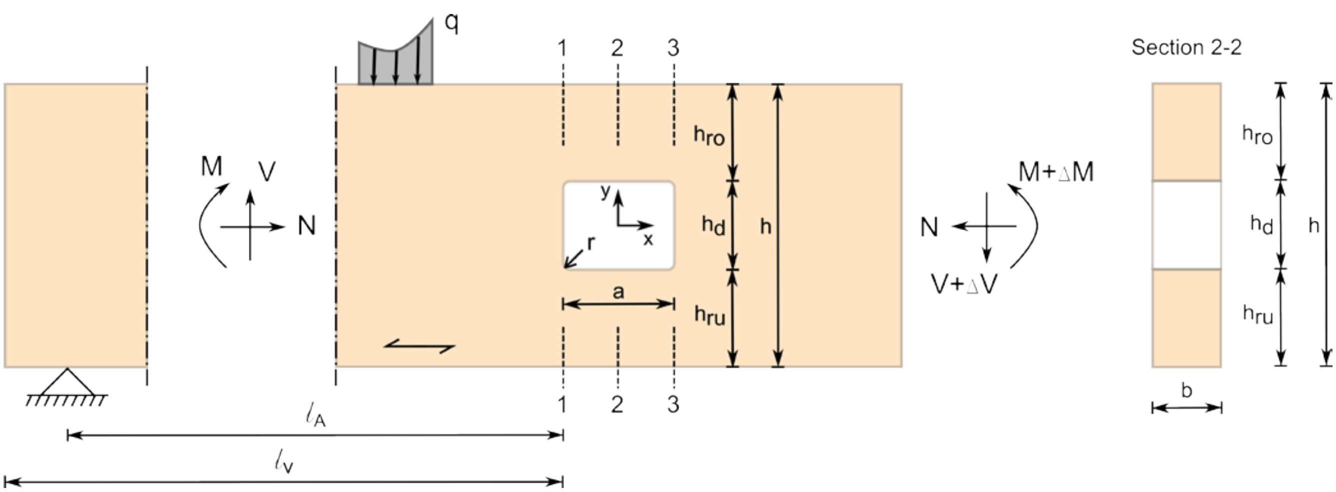

Fig. 1
Dimensional notations of a beam or column with a rectangular hole subjected to combined bending moment, shear and axial force action.

In EC5/NA the relative dimensions of unreinforced rectangular and round holes are restricted to $h_d/h = 0.15$ (note: in the case of round holes, h_d is equal to the hole diameter) and to an aspect ratio (length/depth) of the hole of $a/h_d = 2.7$. In the case of reinforced holes, h_d/h can be up to 0.4. In order to avoid stress singularities, the corners of rectangular holes must be rounded with a radius of at least 15mm. The

ONLINE ISSN 2069-7430
ISSN-L 1841-4737
PRO LIGNO
www.proligno.ro
Vol. 9 N° 4 2013
pp. 50-59

distance between the vertical hole edge closest to the support and the center of the support shall be at a minimum, ℓ_A = h/2. Further, the distance ℓ_V between the closer hole edge and the end grain face of the beam shall not be smaller than the beam depth h.

HOLE DESIGN FOR COMBINED ACTION OF BENDING MOMENT AND SHEAR FORCE

Stresses in the fiber direction

The distributions of normal stresses σ_x in the fiber direction, of normal stresses perpendicular to the fiber direction σ_y and of shear stresses τ_{xy} in the vicinity of rectangular holes subjected to actions of bending moments and shear forces have been presented in detail by Aicher and Höfflin (2003). Several relevant design issues were discussed in detail, such as: i) the dependency of stresses on the ratio of moment vs. shear force M/V, ii) the effect of the radius of the corners and iii) the aspect ratio of the hole a/h_d. Furthermore, the basics of the present hole design EC5/NA were presented and some of its weaknesses were revealed. Additionally, the incorrect design approach given in the former draft EC5 version (FprEN 1995-1-1:2001) was also highlighted. Within the context of this paper, only the basic design equations and a graphical illustration of the distribution of the bending and shear induced normal stresses necessary for understanding the superposition with compression induced normal stresses are given in a comprehensive manner.

Figures 2a-d show exemplarily the distribution of bending and shear induced normal stress σ_x in Sections 1 and 2 at the left edge and at the center of quadratic holes with relative hole sizes h_d/h = 0.15 and 0.3, where both are subjected to a section force ratio M/V = 3h. The presented stress distributions are a result of plane stress finite element analyses. Two material types were considered - the first being a reference isotropic material with a Poisson's ratio of 0.3 and the second having an orthotropic constitutive law with typical stiffness ratios for glulam of E_x/E_y = 30, E_x/G_{xy} = 16 and a Poisson's ratio of v_{xy} = 0.03 (1st index: strain direction). Additionally, the stresses according to the usual beam theory based on the moment of inertia of the net cross-section I_{net} are given as:

$$\sigma_x = \frac{M}{I_{net}} y \quad , \quad \frac{h_d}{2} \leq |y| \leq \frac{h}{2} \tag{1}$$

$$I_{net} = \frac{b}{12}(h^3 - h_d^3) \tag{2}$$

All stress values shown in the figures were normalized with regard to the calculated maximum stress at the extreme fibers (y=h/2) resulting from the corresponding bending moment at the respective section.

The bending stresses in Section 2 (Figs. 2a,b) resemble for both hole to depth ratios those distributions and values anticipated by engineering intuition. The outer fiber normal stress σ_x(y=±h/2) conforms very closely to the beam solution (Eq. 1). Regarding the stress σ_x at the horizontal hole edges at y = ±h_d/2, the FE-computed stress conforms to the analytical solution for small holes, but gets increasingly higher in the case of larger holes with $h_d/h \geq 0.3$. This resembles very closely the stress distributions obtained for round holes by Aicher and Höfflin (2001).

Contrary to the stress distributions in Section 2 through the center of the hole, the bending stresses along Sections 1 and 3, i.e. at the left and right vertical hole edges, show a marked difference versus the analytical beam solution (Figs. 2c,d). This difference results from stress concentrations at the corners. Very roughly, the outer fiber bending stresses $\sigma_{x,1,3}$(y=±h/2) are almost equal to the analytical solution based on the net cross-section up to hole depth ratios of h_d/h = 0.15; for larger h_d/h ratios, stresses σ_x(y=±h/2) are increasingly below the beam solution. In contrast, at the hole edges y = ±h_d/2, a marked stress increase versus simple beam theory occurs within a considerable area. The increase in the normal stress $\sigma_{x,1,3}$(y=±h_d/2) can be expressed by a stress concentration factor $\eta_{1,3}$ which depends considerably on the hole to depth ratio h_d/h. For the considered material type with orthotropic constitutive relations this factor is given approximately in Eq. 3. Therefore, the stresses at the hole edges can be calculated as shown in Eq. 4.

$$\eta_{1,3} = 3\frac{h_d}{h} \tag{3}$$

$$\sigma_{x,1,3}(y=\pm\frac{h_d}{2})=\frac{M_{1,3}}{I_{net}}(\pm\frac{h_d}{2})\eta_{1,3} \qquad (4)$$

Since the stress increase is restricted to a rather confined area, the shape of the stress contour has to be taken into consideration when effects of yielding at the compression corners of the hole or quasi-brittle behavior at the tensile corners are considered in the limit states design.

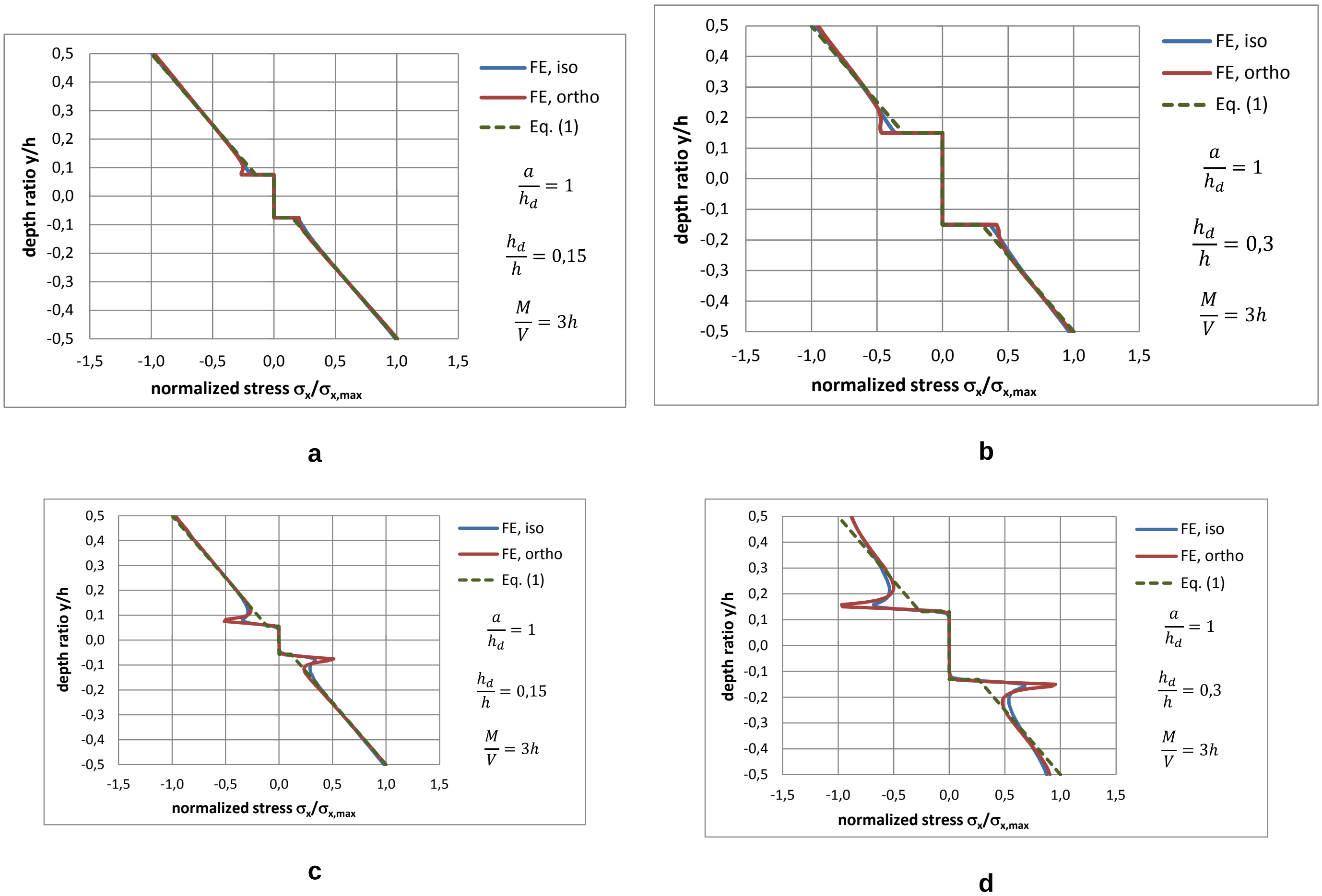

Fig. 2
Effect of relative hole size on normal stresses in fiber direction in a beam subjected to bending moment and shear force action: Section 2: a - hd/h=0.15; b - hd/h=0.3
Section 1: c - hd/h=0.15; d - hd/h=0.3.

Stresses perpendicular to fiber direction

Regarding normal stresses perpendicular to the fiber direction σ_y, tensile and compression stress fields occur at diagonally opposite corners of the hole (Fig. 3). In the case of a positive bending moment and related shear forces, tensile stresses occur at the diagonally opposite lower left and upper right corner of the hole, whereas the other corners are subjected to compression stress fields. The magnitude and similarity of the σ_y stress distributions at the four corners depend strongly on the hole depth ratio h_d/h and on the ratio of bending moment versus shear force M/V. All stress values shown in the figures were normalized with regard to the calculated maximum stress resulting from the corresponding bending moment at the respective section (ℓ_A and ℓ_A+a).

According to EC5/NA the resultant maximum tensile force bound to the combined action of shear force V and moment M in the corner areas is (V and M at the respective vertical hole edges, or Sections 1 and 3)

$$F_{t,90} = F_{t,V} + F_{t,M} = V\frac{h_d}{4h}\left[3-(\frac{h_d}{h})^2\right] + M\frac{0{,}008}{h_r} \quad . \qquad (5)$$

In most realistic design situations the contribution from the shear force V labeled as $F_{t,V}$ in the above equation is by far the dominating action. For design verification it suffices to consider only the highest stressed paths stretching horizontally at y = ±h_d/2 from the corners as shown in Figs. 4a,b. In EC5/NA, a triangular stress distribution with a maximum value of

$$\sigma_y = \sigma_{t,90,\max} = \frac{2F_{t,90}}{b \cdot l_{t,90}} \quad . \qquad (6)$$

has been assumed and in an approximation, the stress distribution length was fixed as

$$l_{t,90} = 0{,}5(h_d + h) \; . \qquad (7)$$

It has been shown that the stress distribution length $l_{t,90}$ specified by Eq. (7) is far too long, thus reducing $\sigma_{t,90,\max}$ unduly (Aicher and Höfflin, 2001 and 2003). This is also clearly depicted in Figs. 4a,b. In a more realistic approach, $l_{t,90}$ should be roughly reduced by 50%, thus increasing $\sigma_{t,90,\max}$ by a factor of 2.

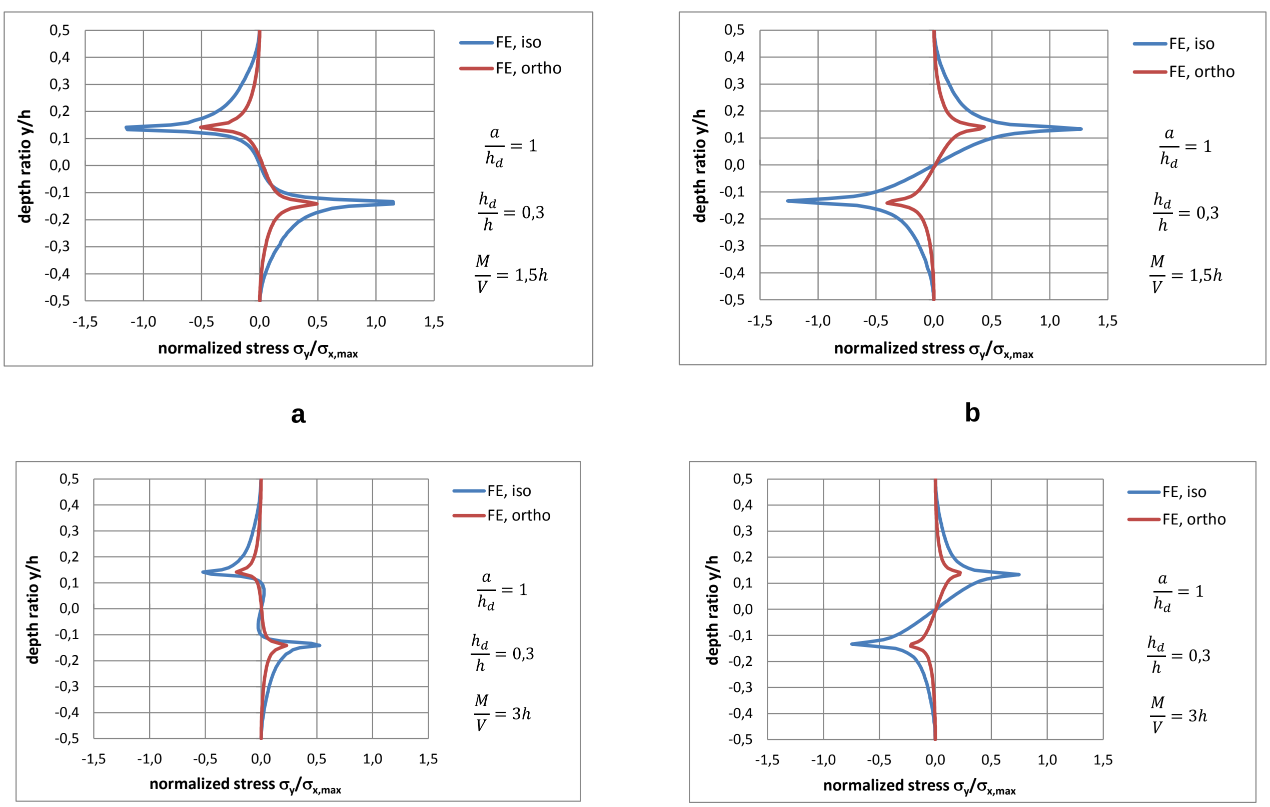

a b c d

Fig. 3

Effect of the moment to shear force ratio on the normal stresses perpendicular to fiber direction at the left - and right-hand side hole edges (tension as positive)

ratio M/V=1.5h: a - Section 1; b - Section 3

ratio M/V=3.0h: c - Section 1; d - Section 3.

ONLINE ISSN 2069-7430
ISSN-L 1841-4737
PRO LIGNO
www.proligno.ro
Vol. 9 N° 4 2013
pp. 50-59

HOLE DESIGN FOR AXIAL COMPRESSION FORCE ACTION

Stresses in the fiber direction

Fig. 5 depicts the considered loading case of a glulam beam subjected to pure compression parallel to the beam and fiber axis. At a sufficient distance from the vertical hole edges, roughly conforming to 3·a, the uniformly distributed nominal compression stress $\sigma_{x,nom} = N_x/(b \cdot h)$ occurs.

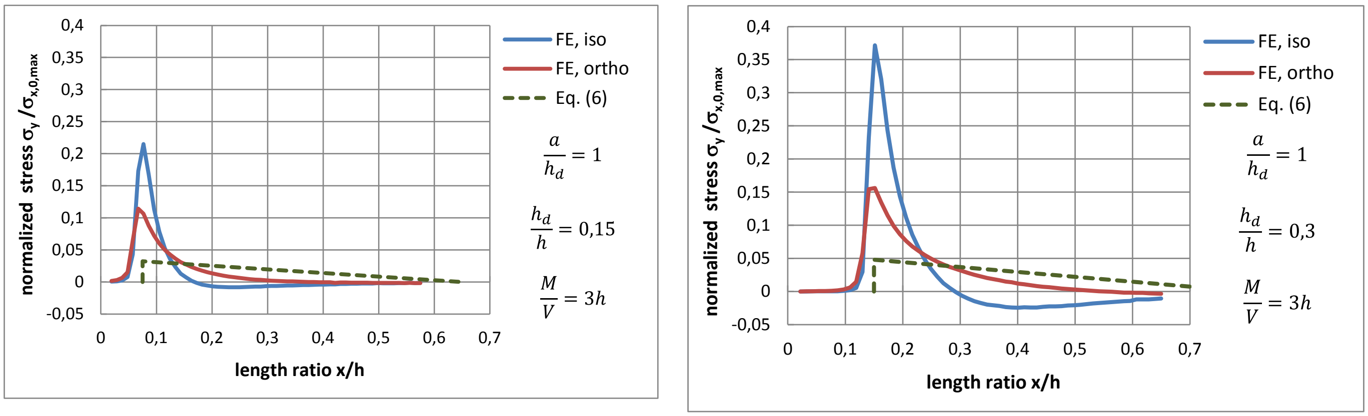

a

b

Fig. 4
Effect of the hole size on the normal stresses perpendicular to fiber direction at the top right hole corner in a beam subjected to moment and shear force action (tension as positive)
a - h_d/h=0.15; b - h_d/h=0.3.

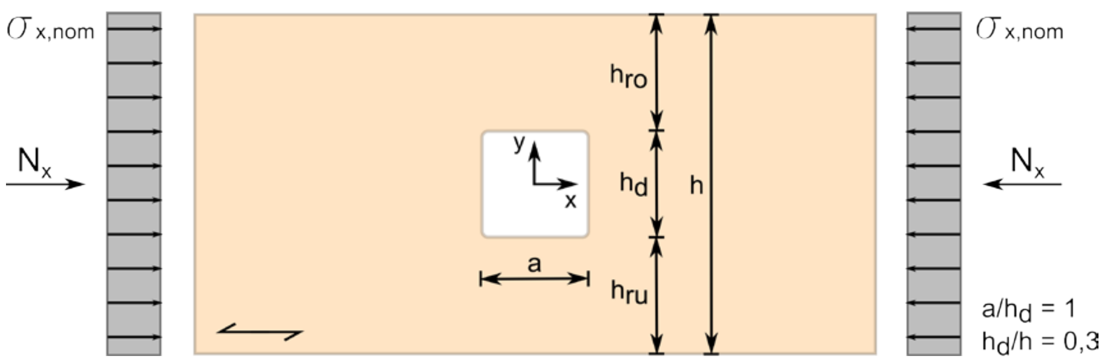

Fig. 5
Dimensional notations of a beam or column with a square hole subjected to pure compression in beam and fiber direction.

In a very crude assumption, the compression stress determination in Section 2 at the hole center might be performed by means of the net area yielding in case of a symmetrically placed hole ($h_r = h_{ru} = h_{ro}$)

$$\sigma_{x,net} = \frac{N_x}{A_{net}} = \frac{N_x}{b\,(h - h_d)} = \sigma_{x,nom}\left(1 + \frac{h_d}{2h_r}\right) . \qquad (8)$$

A more realistic engineering approach is based on the understanding that a uniform redistribution of the stresses σ_x that cannot be transferred through the hole area h_d to the upper and lower cross-sections with depths h_r is not possible, at least not for realistic hole aspect ratios. More appropriately, a triangular redistribution

ONLINE ISSN 2069-7430
ISSN-L 1841-4737

PRO LIGNO Vol. 9 N° 4 2013
www.proligno.ro pp. 50-59

of the additional stresses along h_r can be assumed, yielding at the horizontal hole edges $y = \pm h_d/2$ and at the outer fibers $y = \pm h/2$ the maximum and minimum stresses

$$\sigma_x\left(y = \pm\frac{h_d}{2}\right) = \sigma_{x,nom}\left(1 + \frac{h_d}{h_r}\right) \tag{9a}$$

$$\sigma_x\left(y = \pm\frac{h}{2}\right) = \sigma_{x,nom} \quad . \tag{9b}$$

Both engineering assumptions quantified by Eqs. (8) and (9a,b) are compared in Figs. 6a,b to finite element computed stress distributions for two square hole configurations h_d/h = 0.15 and 0.3. Note: All stresses are given normalized to the negative quantity $\sigma_{x,nom}$. Both figures reveal very uneven compression stress distributions with high stress peaks at the hole edges $y = \pm h_d/2$ which are considerably more pronounced in the case of the material which follows orthotropic constitutive law. This is an immediate consequence of the very low normal stiffness perpendicular to the fiber direction and the low shear rigidity when related to MOE parallel to the fiber direction, $E_y = E_x/30$, $G_{xy} = E_x/20$, which hinder a more effective stress redistribution to the beam parts further away from the hole. This effect is clearly evident from the graphs for both depicted hole to depth ratios h_d/h = 0.15 and 0.3 where the isotropic solution shows throughout a considerably lower stress peak but higher stresses further away from the hole.

It is further apparent from the graphs that the crude assumption of a constant value $\sigma_{x,net}$ for assessment of the stress level leads to an underestimation of the true stress distribution adjacent to the hole edges and an overestimation of the true stress distribution adjacent to the outer beam fibers. Contrarily hereto, the trapezoidal stress distribution defined by Eqs. (9a,b) gives a considerably better representation of the true orthotropic stress distribution and in the case of h_d/h = 0.3, a fairly close approximation to the isotropic results. Nevertheless, for smaller hole to depth ratios the trapezoidal distribution also leads to a severe underestimation of the maximum stress at the hole edge. Thus, in the case of h_d/h = 0.15, the true stress is almost two times higher as compared to the solution predicted by Eq. (9a).

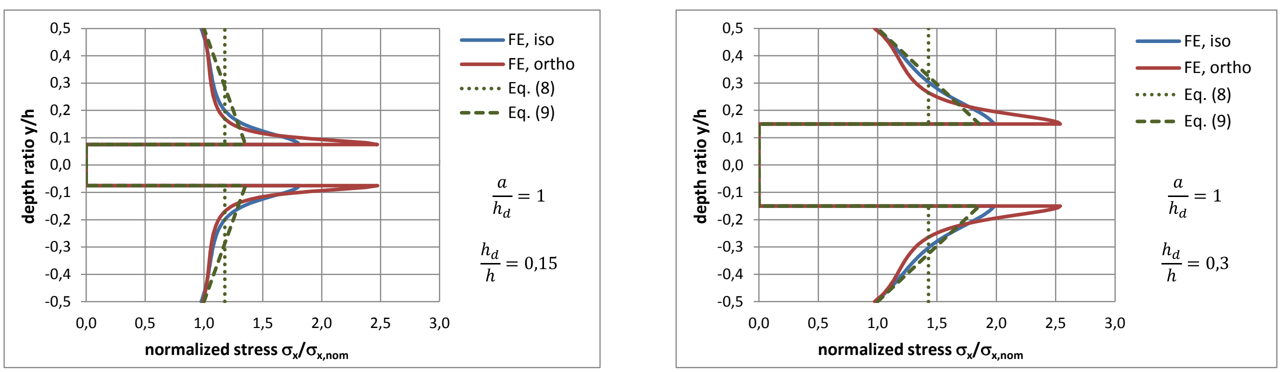

a b

Fig. 6
Effect of the hole size on the distribution of normal stresses in fiber direction in a section through the center of the hole in a beam subjected to pure axial force action
a - h_d/h=0.15; b - h_d/h=0.3.

Stresses perpendicular to the fiber direction

It is evident that the compression stresses $\sigma_{x,nom}$ distributed uniformly along the hole depth h_d at a sufficient distance from the hole, have to diverge from the axial direction x in order to flow around the hole. As both compression stress resultants $F_{hd/2} = \sigma_{x,nom}\cdot b\cdot h_d/2$ at each of the Sections 1 and 3 have to be transferred through the remaining cross-sections with depth h_r, a resultant force which is very roughly $F_{r,hd/2} = F_{hd/2}/\cos\alpha$ must act, having a certain angle α oriented towards the outer beam edges at $y = \pm h/2$. Consequently, forces $F_{t,90}$ perpendicular to the beam axis arise as shown schematically in Fig. 7, which may be roughly assessed as $F_{t,90} = \tan\alpha\cdot F_{hd/2}$. The tensile stresses related to forces $F_{t,90}$ show a typical distribution along the beam length in front of the hole as illustrated schematically in Fig. 7. Figs. 8a,b show the stresses σ_y in section y = const = 0, i.e. at mid-depth for two different hole to beam depth ratios h_d/h = 0.15 and 0.3. The maximum tensile stresses occur at the vertical hole edges and abate sharply away from the hole.

The distribution of stresses perpendicular to the fiber direction along Sections 1 and 3 is shown in Figs. 9a,b for $h_d/h = 0.15$ and 0.3. Both figures depict the stresses for the case of orthotropic material properties appropriate for glulam as well as for the reference isotropic case. The graphs show that the tensile stresses are almost constant along the entire hole depth h_d. At the corners of the hole, the stresses change within a very small area from tension into compression with a pronounced stress peak immediately beyond the hole edge at $y \geq |\pm h_d/2|$. Additionally, the graphs reveal an enormous difference regarding the considered constitutive laws. In case of isotropy, the tensile stress $\sigma_{y,max}$ at mid-depth and almost throughout the entire hole depth is closely equal in magnitude to the applied compression stress, i.e. $\sigma_{y,max} \approx |\sigma_{x,nom}|$. In contrast, in the case of the orthotropic material law the maximum tensile stress is considerably lower and conforms to about $\sigma_{t,90,max} = \sigma_{y,max} = 0.2\sigma_{x,nom}$ irrespective of the ratio h_d/h. The maximum compression stress peaks adjacent to the corners, slightly beyond $y > |\pm h_d/2|$ is $\sigma_{c,90,max} = 0.15\sigma_{x,nom}$.

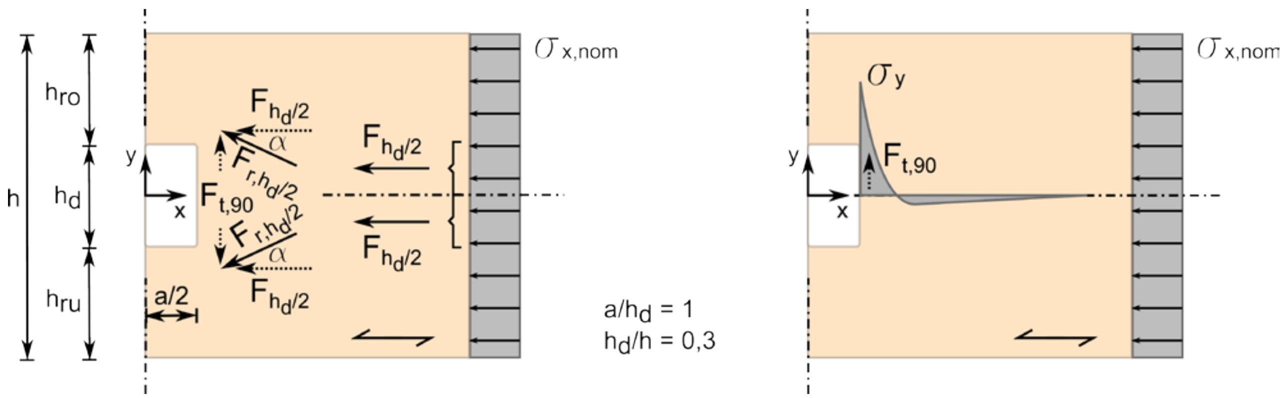

Fig. 7
Illustrations of the stress flow deviation around a hole and the resulting tensile stresses in direction perpendicular to fiber.

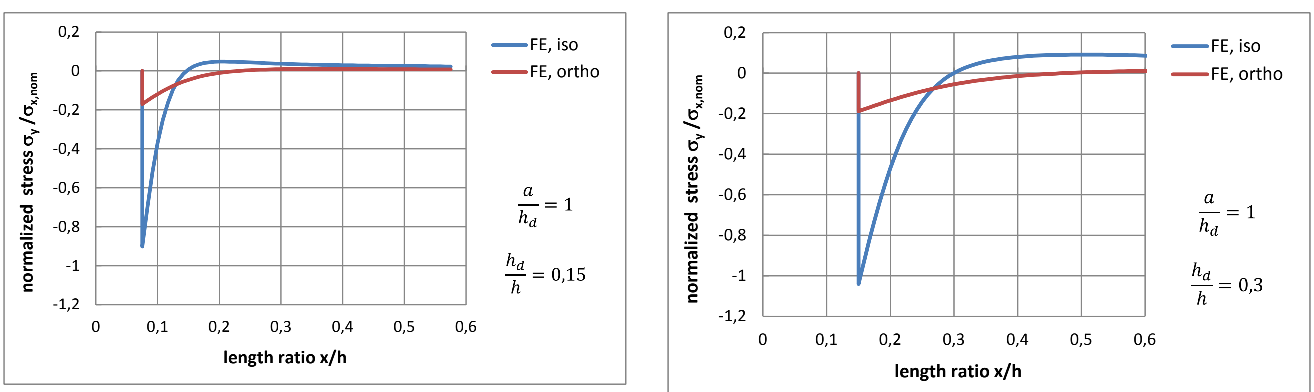

a   b

Fig. 8
Effect of the hole size on the distribution of normal stresses perpendicular to the fiber direction in a section through the center of the hole in a beam subjected to pure axial force action
a - h_d/h=0.15; b - h_d/h=0.3.

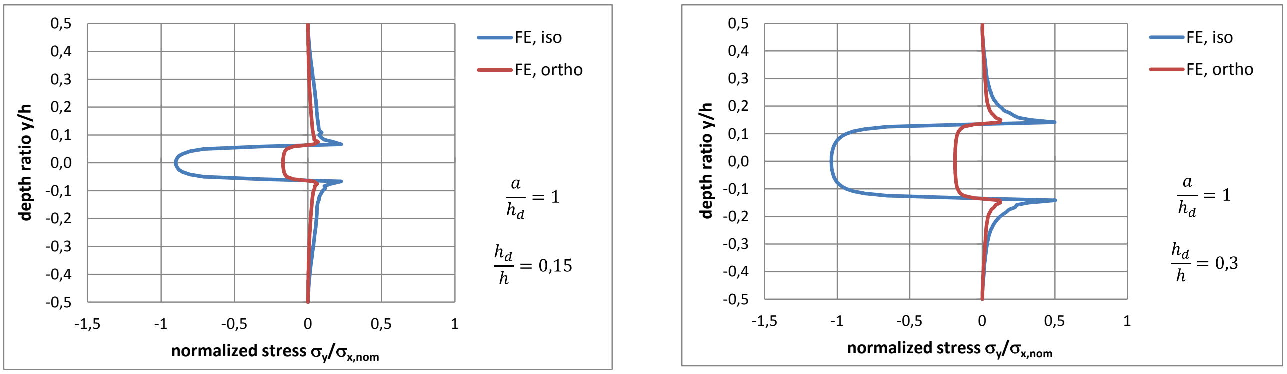

a

b

Fig. 9

Effect of the hole size on the distribution of normal stresses perpendicular to fiber direction in a section at the edge of the hole in a beam subjected to pure axial force action

a - $h_d/h=0.15$; b - $h_d/h=0.3$.

COMBINED ACTION OF MOMENT, SHEAR AND AXIAL FORCE

For the case of the combined action of an axial compression force and bending in a beam column with a rectangular hole, the above given extreme values have to be superimposed. Hereby the stress signs have to be considered appropriately as in the case of moment action, where the position of the corners subjected to tension or compression perpendicular to the fiber direction depends on the sign of the moment. Depending on the respective section force magnitudes, it may easily be the case that the compression stress along the horizontal hole edges and especially at one of the four hole corner becomes considerably larger than the design compression strength $f_{c,0,d}$ parallel to the fiber direction, necessitating considerations on stress redistribution via plastic yielding. Furthermore, the tensile stresses perpendicular to the fiber along the vertical hole edges will in general be significantly beyond the very low design tensile strength $f_{t,90,d}$, which for all glulam strength classes given in FprEN 14080:2013 is $f_{t,90,d} = 0.5 \cdot k_{mod}/\gamma_M$, where k_{mod} is the modification factor for climate and load duration and γ_M the nationally determined partial safety factor. In case of larger beam and hole depths, an additional size effect reduction factor for $f_{t,90,d}$ has to be considered. The magnitude of the size effect can be derived from a Weibull integration of the tensile stress field as shown in Aicher and Höfflin (2004) and Aicher *et al.* (2007). As an approximation, a square root size influence as specified in EC5/NA for hole design may be assumed. As the failure mode in tension perpendicular to the fiber direction is brittle, a design verification result of $\sigma_{t,90,d} > f_{t,90,d}$ necessitates apt reinforcement provisions, for instance by means of self-tapping screws. Alternatively it has to be verified that the cracks parallel to the grain starting from the vertical hole edges remain local and are not influencing the global structural safety of the load-bearing element.

CONCLUSIONS

The paper revealed quantitatively that axial compression loading of a glulam beam incorporating a rectangular hole changes considerably the design relevant stresses obtained by means of analytical beam solutions for an isotropic material. The compression stresses parallel to the fiber direction are greatly increased in a considerably wide band area adjacent to the horizontal hole edges. The tensile stresses perpendicular to the fiber in front of the vertical hole edges resulting from the deviation of the stresses parallel to the fiber due to the existence of the hole, are reduced in the case of an orthotropic material such as wood to about 20% as compared to the isotropic solution. Nevertheless, due to the very low tensile strength perpendicular to the fiber direction, a high probability of crack formation adjacent to the hole edges still exists.

Regarding the superposition of stresses from moment, shear force and axial compression, it is evident from the presented equations that the locations of potential yielding or brittle fracture in the vicinity of rectangular holes in glulam depend pronouncedly on the signs of moment and shear force and on the ratio of axial compression versus moment and shear force. The issue of compression yielding and cracking in tension perpendicular to the grain in the vicinity of holes is considered in ongoing investigations.

REFERENCES

Aicher S, Höfflin L (2001) Round holes in glulam members. Part 1: Analysis. Bautechnik 78(10):706–715 (in German)

Aicher S, Höfflin L (2003) Design of rectangular holes in glulam beams. Otto Graf Journal 14:211-229

Aicher S, Höfflin L (2004) New design model for round holes in glulam beams. Proceedings of 8th World Conference on Timber Engineering, 2004, Vol. 1, pp. 67-72, Lahti, Finland

Aicher S, Höfflin L, Reinhardt HW (2007) Round holes in members made of glued laminated timber: Part 2 Load capacity and design, Bautechnik 2007, 84(12):867-880

FprEN 1995-1-1:2001 Eurocode 5: Design of timber structures – Part 1-1: General rules and rules for buildings, Final draft prEN 1995-1-1, CEN/TC 250/SC5 N 173, 2001-04-09

EN 1995-1-1:2010 Eurocode 5: Design of timber structures – Part 1-1: General – Common rules and rules for buildings; German version EN 1995-1-1:2004 + AC:2006 + A1:2008

DIN EN 1995-1-1/NA:2010 National Annex – Nationally determined parameters – Eurocode 5: Design of timber structures – Part 1-1: General – Common rules and rules for buildings

FprEN 14080:2013 Timber structures – Glued laminated timber and glued solid timber – Requirements